

Damage Thresholds for New Collimator Materials, Experiment Detectors and SC Magnet Components

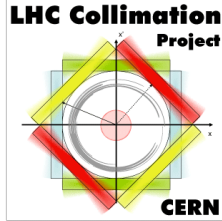
F. Carra (EN-MME), C. Bertella (EP), A. Sbrizzi (EP), D. Wollmann (TE-MPE)
With contributions from colleagues of EN-MME, BE-ABP, EN-STI, TE-MPE, EP

MPP Workshop 2019

Chateau de Bossey

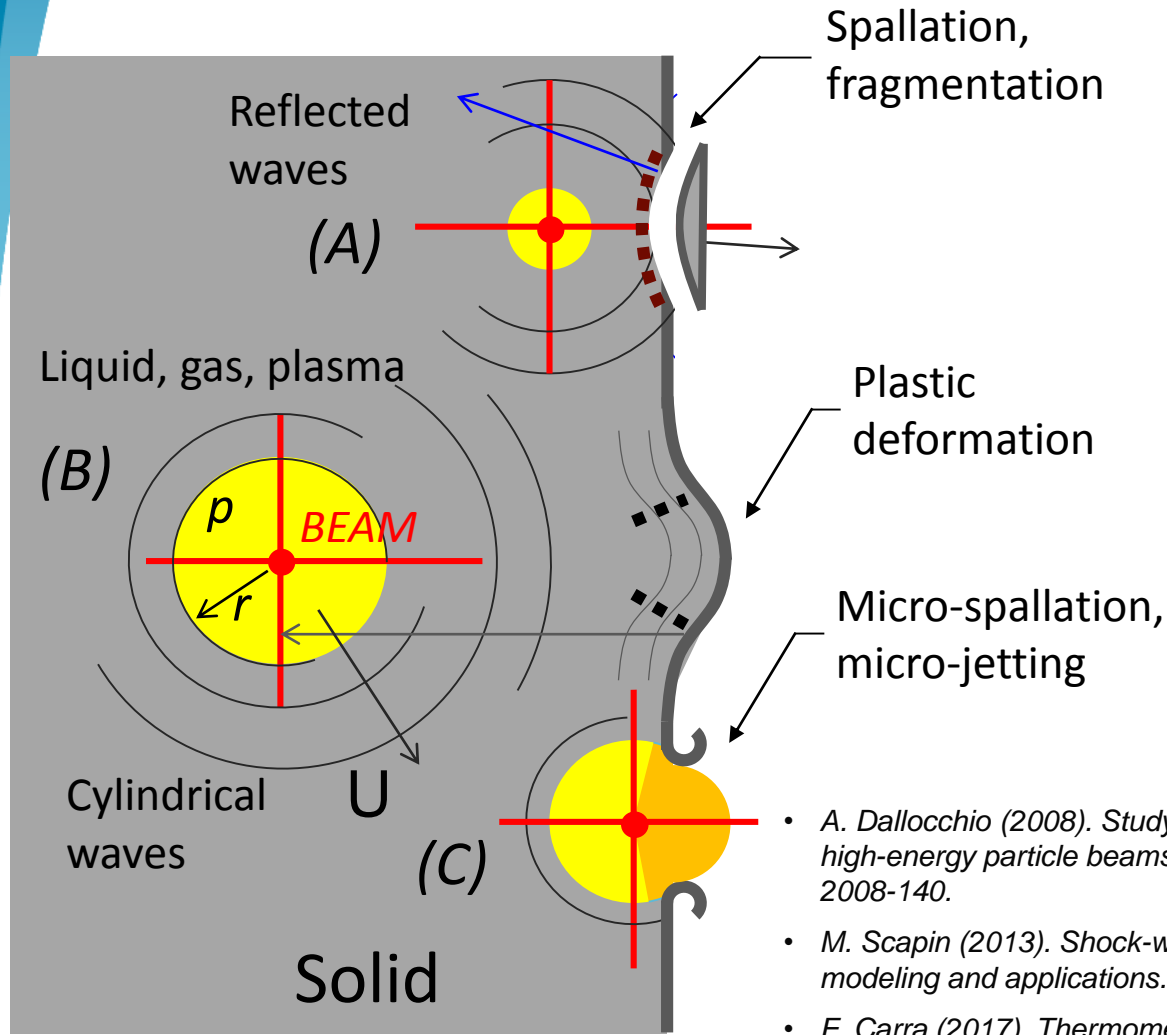
May 7th, 2019

Outline



- Introduction
 - Particle beam – matter interactions
 - Damage mechanisms
- Collimator materials
 - HiRadMat experiments
 - Damage thresholds
- SC magnet components
- ATLAS detectors
- Conclusions

Introduction to beam damage



Cylindrical spreading loss

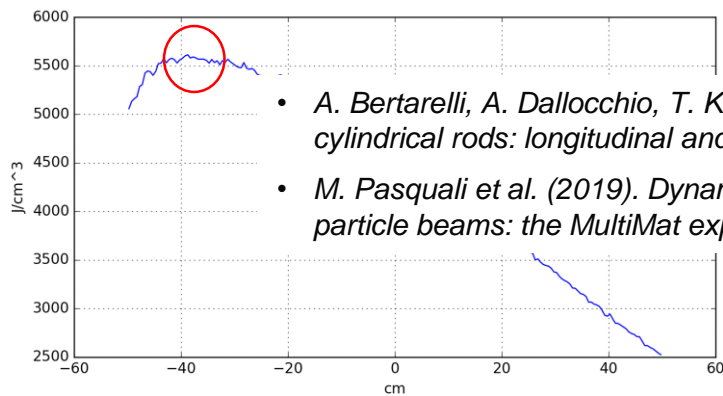
- Far from the impact point
 - $P \propto r^{-1/2}$ (for spherical: r^{-1})
 - $E \propto r^{-1}$ (for spherical: r^{-2})
- Close to the impact
 - Logarithmic singularity

- A. Dalocchio (2008). Study of thermomechanical effects induced in solids by high-energy particle beams: analytical and numerical methods. CERN-THESIS-2008-140.
- M. Scapin (2013). Shock-wave and high strain-rate phenomena in matter: modeling and applications. PhD thesis, 10.6092/polito/porto/2507944.
- F. Carra (2017). Thermomechanical Response of Advanced Materials under Quasi Instantaneous Heating. PhD thesis, <https://zenodo.org/record/1414090>.

Introduction to beam damage

- Damage is triggered by the energy absorbed by the material
- Two parameters controlling the damage:
 - Energy density peak** e_p (J/cm³) → localized effects, the onset of damage, ...
 - Average energy per target section** \bar{e}_s (J/cm³) → global response of the target, the damage far from the impact, ...

Energy density peak (e_p)

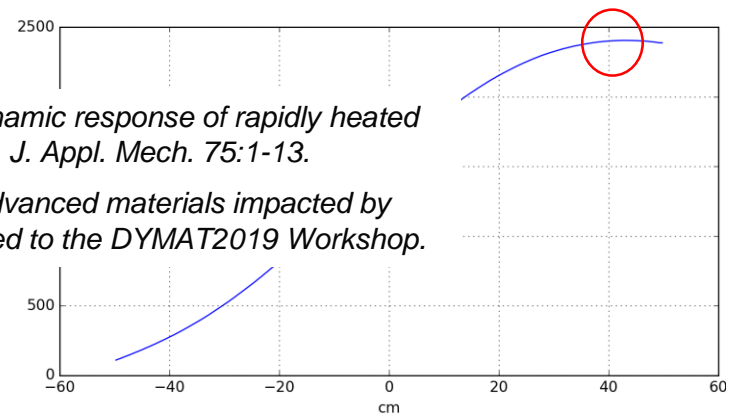


- A. Bertarelli, A. Dallochio, T. Kurtyka (2008). *Dynamic response of rapidly heated cylindrical rods: longitudinal and flexural behavior*. *J. Appl. Mech.* 75:1-13.
- M. Pasquali et al. (2019). *Dynamic response of advanced materials impacted by particle beams: the MultiMat experiment*. Submitted to the DYMAT2019 Workshop.

$$T_p = \frac{e_p}{\rho c_p} > T_{lim} \rightarrow \text{DAMAGE}$$

$$\varepsilon_p = f(\alpha T_p) > \varepsilon_{lim} \rightarrow \text{DAMAGE}$$

Average energy on the most loaded section (\bar{e}_s)

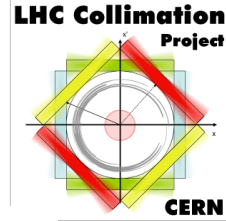


$$\bar{e}_s = \bar{E}_s / A$$

$$\bar{T}_s = \frac{\bar{e}_s}{\rho c_p}$$

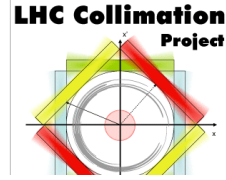
$$\varepsilon_s = 2\alpha \bar{T}_s > \varepsilon_{lim} \rightarrow \text{DAMAGE}$$

Collimator damage thresholds



- **Three damage thresholds** defined for collimator materials.
 - Introduced for metallic (ductile) materials see MPP Workshop 2013, Annecy. Extended here to graphitic ones.
 - Defined as a function of the effect on the collimator behaviour.
- **Threshold 1:** onset of damage, with no need to activate the 5th axis.
 - Ductile materials: onset of plasticity.
 - Graphitic materials: crack initiation, local material ablation.
- **Threshold 2:** damage to the surface requiring correction with the 5th axis.
 - Ductile materials: it usually involves heavy plastic deformation and/or ejecta generation.
 - Graphitic materials: pseudo-plastic deformation, internal delamination, important material ablation, ...
- **Threshold 3:** damage cannot be corrected with 5th axis anymore.
 - Ductile materials: significant material erosion and plastic deformation in the jaw, no more flat surface close to the impact.
 - Graphitic materials: fracture of the blocks jeopardizing the structural integrity, complete block face delamination with loss of the flatness.

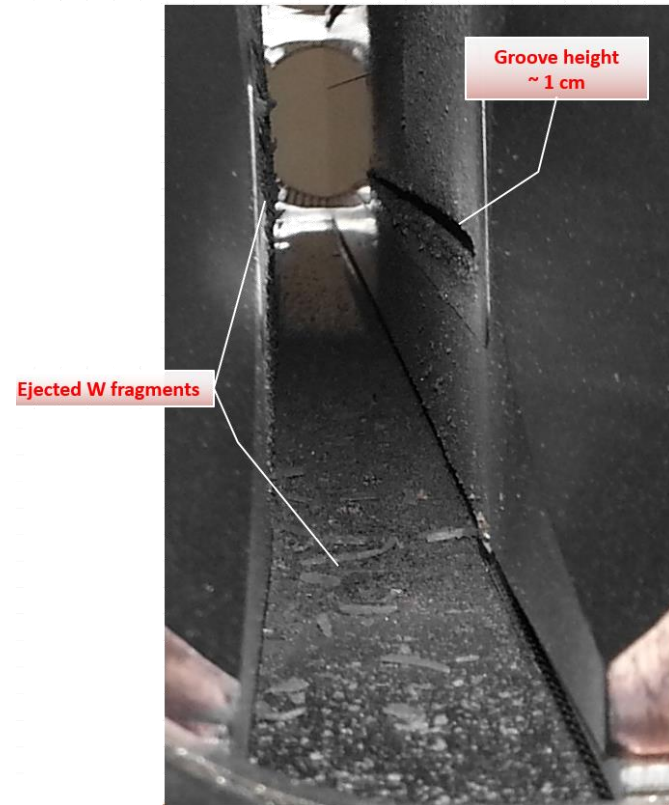
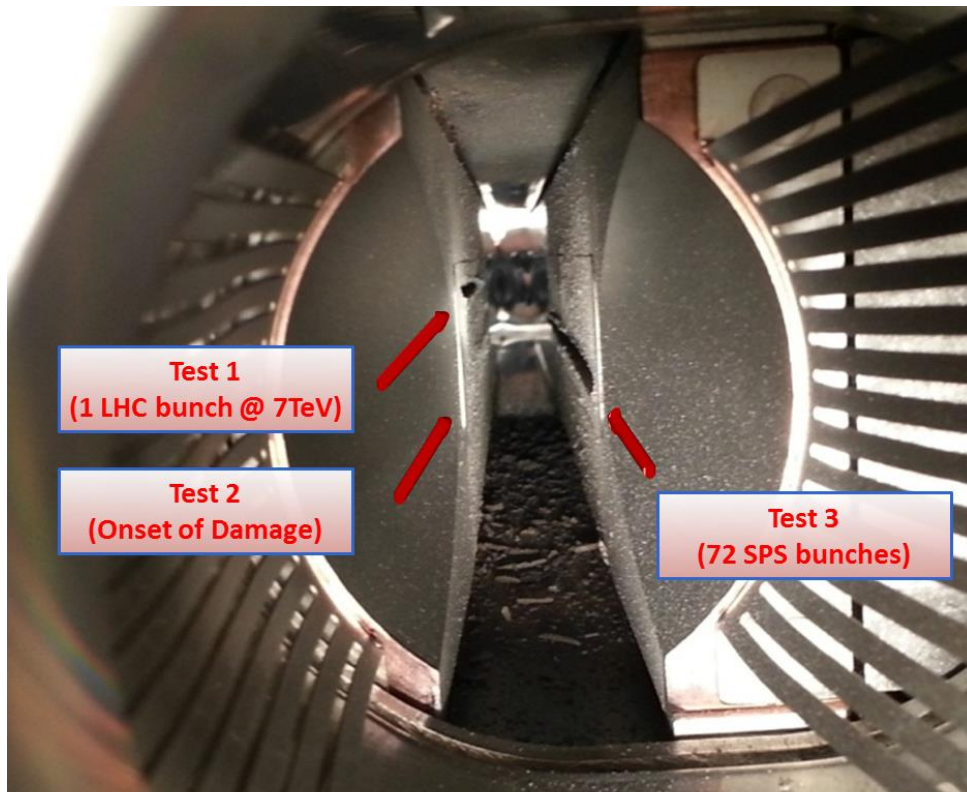
Collimator materials



- The evaluation of material response to beam impact is done in two ways:
 - **Numerical simulations** (FLUKA + ANSYS, Autodyn, LS-Dyna)
 - **Experimental tests** (HiRadMat: on full-scale devices or on simple geometry targets)
- The damage thresholds are estimated with a **combination of the two techniques**
- **HiRadMat experiments** on collimator materials and devices:
 - HRMT-09 (2012): TCT collimator (Inermet180)
 - HRMT-14 (2012): collimator material samples (cylinders and half-moons)
 - HRMT-23 (2015): LHC and HL-LHC collimator jaws (CFC, MoGr, CuCD)
 - HRMT-21 (2017): Rotatable collimator (Glidcop) → *see backup slides*
 - HRMT-36 (2017): collimator material samples (rods, uncoated and coated)

HRMT-09 (2012)

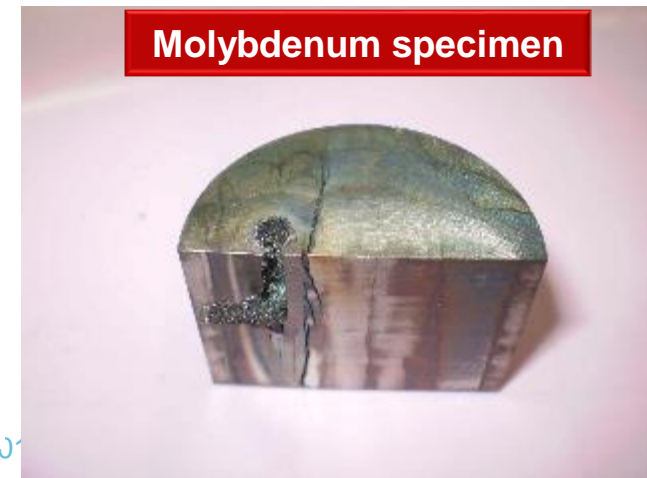
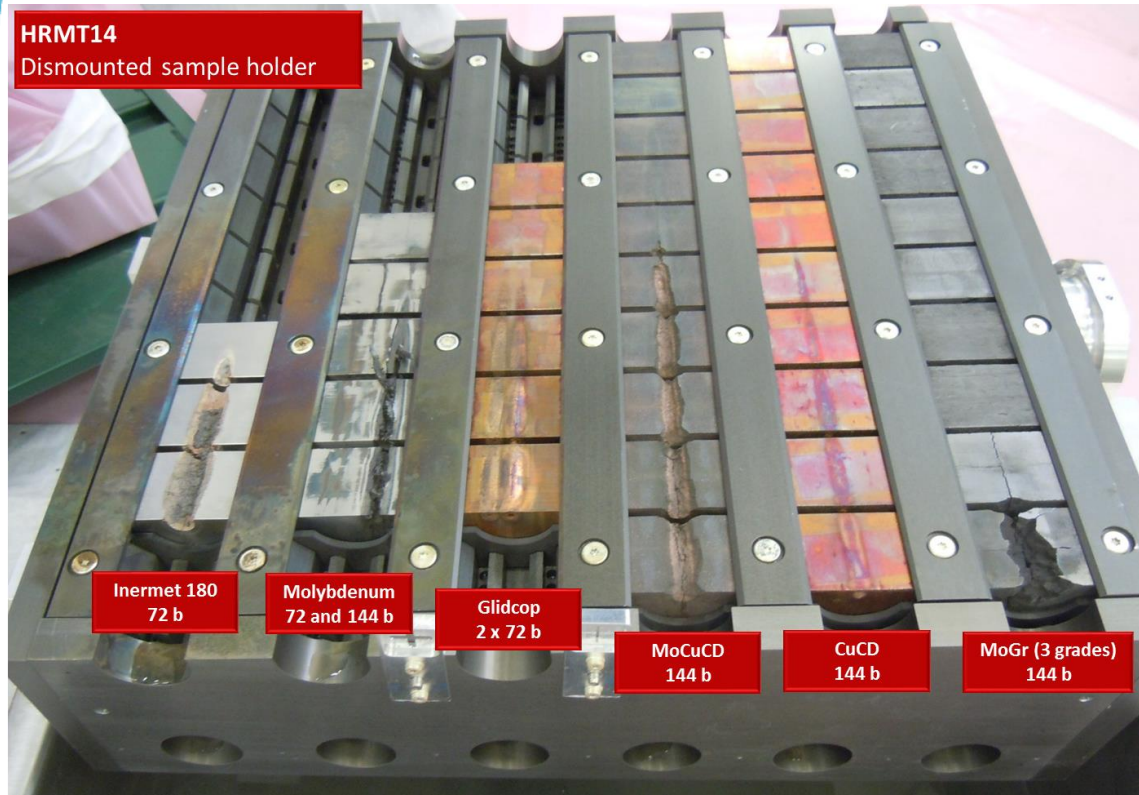
- Testing of a spare TCT collimator
- Allowed to derive **damage limits for tertiary collimator jaws** (Inermet180)
- Highlighted **additional potential machine protection issues on top of mechanical damage**, due to projection of fragments and dust (UHV degradation, contamination of vacuum chambers, complication of dismounting procedure)



- M. Cauchi (2014). High energy beam impact tests on a LHC tertiary collimator at the CERN high-radiation to materials facility. *Phys. Rev. ST Accel. Beams* 17, 021004. May 2019

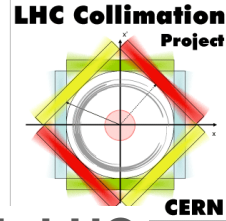
HRMT-14 (2012)

- Test of specimens from 6 different materials: Inermet180, Mo, Glidcop, MoCuCD, CuCD, and MoGr (very old grade with high density, 5.4 g/cm^3)
- Allowed **characterization of materials of interest for collimators**
- **Tuning of numerical models, with very good benchmarking between measurements and simulations**

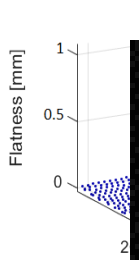


- A. Bertarelli et al. (2013). An experiment to test advanced materials impacted by intense proton pulses at CERN HiRadMat facility. *Nucl. Instr. Meth. Phys. Res. B* 308:88–99.

HRMT-23 (2015)



- Test on three collimator jaws: CFC (LHC design), MoGr and CuCD (HL-LHC design)



HL design

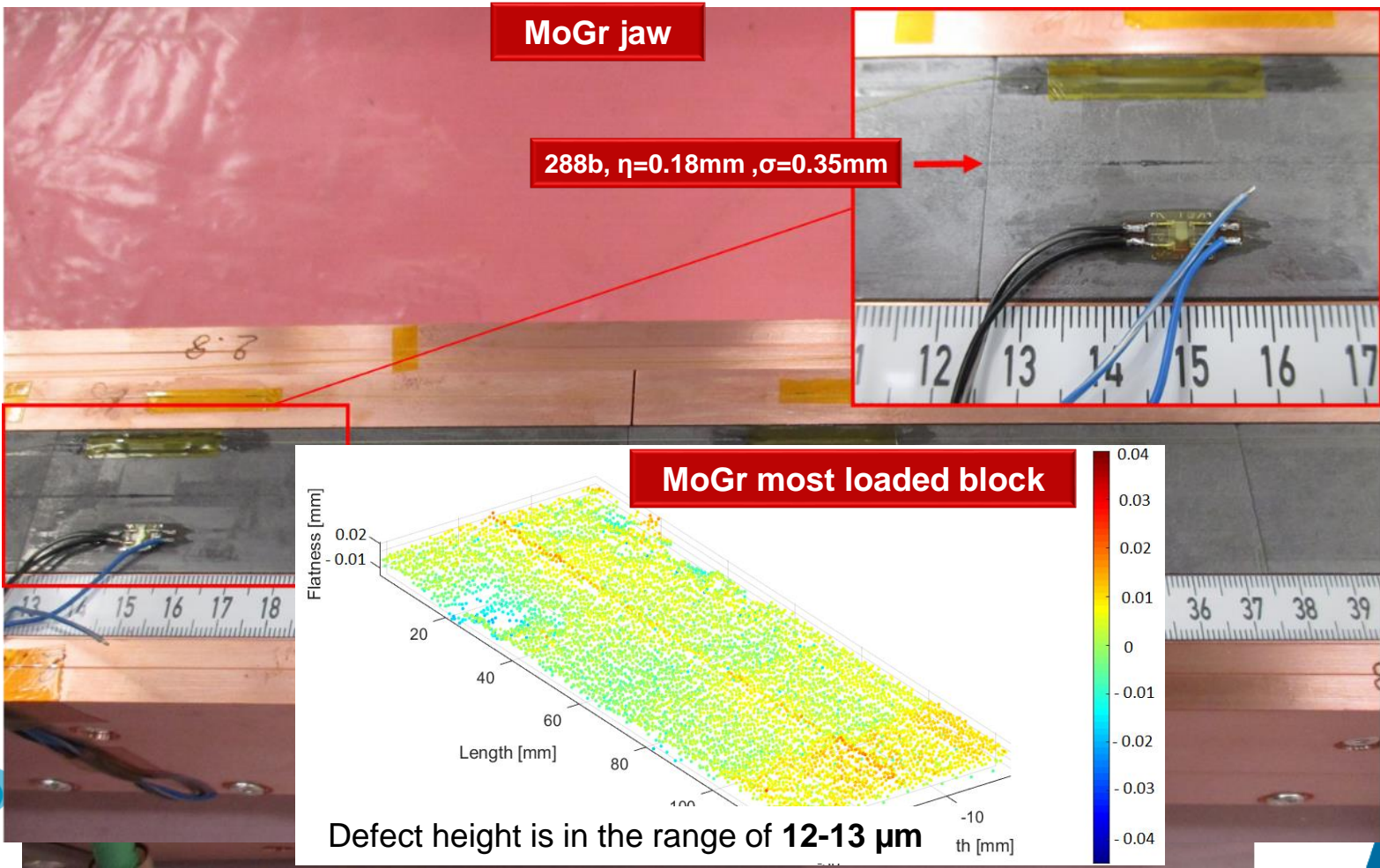
and CFC: we

CuCD jaw

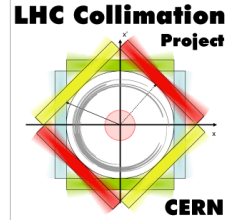
- F. Carra (2017). *Thermomechanical Response of Advanced Materials under Quasi Instantaneous Heating*. PhD thesis, <https://zenodo.org/record/1414090>.
- G. Gobbi et al. (2019). *Novel LHC collimator materials: High-energy Hadron beam impact tests and non-destructive post-irradiation examination*. *Journal of Mechanics of Advanced Materials and Structures*.
- F. Carra et al. (2019). *Mechanical robustness of HL-LHC collimator designs*. Accepted in IPAC19, Melbourne, Australia.

HRMT-23 (2015)

- In the case of CFC and MoGr, minor traces visible after the grazing impacts at 144b and 288b (spallation: onset of damage \rightarrow *threshold 1*)
- Deeper impacts (even at 288b) \rightarrow no damage (smaller tensile wave at surface)
- No \bar{e}_s -induced damage on downstream blocks



HRMT-36 (2017)



#	Material	Density [g/cm ³]	Coated	Coating Material
1	IT180	18.0	✗	
2	Ta10W	16.9	✗	
3	Ta2.5W	16.7	✗	
4	TZM	10.0	✗	
5	CuCD IFAM	5.40	✗	
6	CuCD RHP	5.40	✗	
7	SiC	3.21	✗	
8	MG-6403Fc	2.54	✓	5μm TiN
9	ND-7401-Sr	2.52	✗	
10	MG-6530Aa	2.50	✓	2μm Cu
11	MG-6541Fc	2.49	✓	8μm Mo
12	TPG	2.26	✗	
13	TG-1100	2.19	✗	
14	R4550	1.90	✓	2μm Cu
15	CFC AC150K	1.88	✓	8μm Mo
16	Ti6Al4V (AM)	1.62	✗	
17	CFOAM	0.40	✗	
18	Al 6082-T651 (UoHud)	2.70	✗	

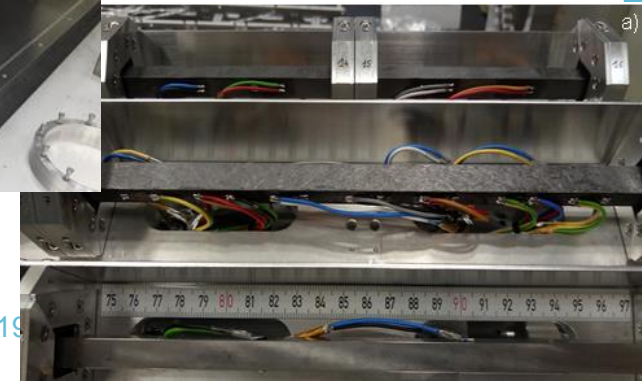
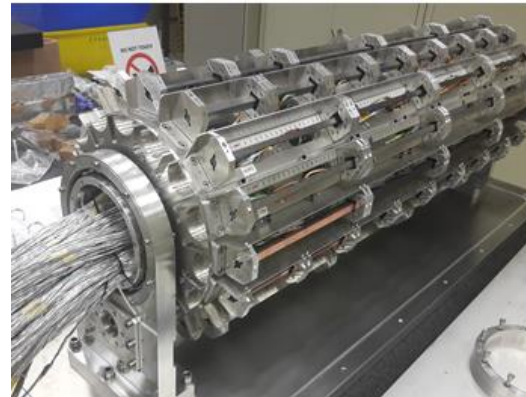
high density

medium density

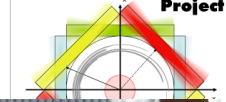
low density

Dedicated setup

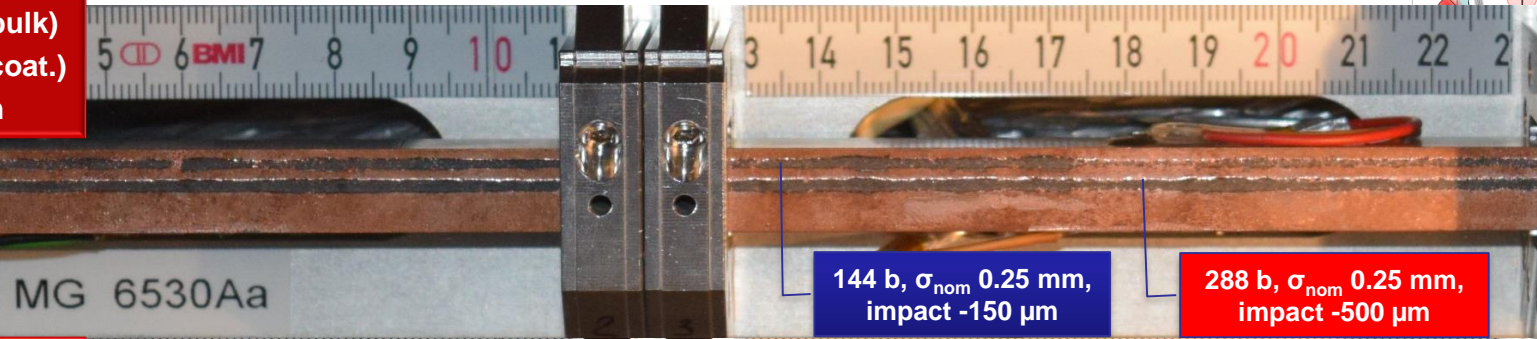
- Test on 16 target stations, including **coated and uncoated material targets (rods)** and electronic devices
- Specimen geometry chosen to:
 - Generate easily detectable **uniaxial signals**
 - Enhance \bar{e}_s (factor 2-3 above HL-LHC!)** thanks to sample section $\sim 1/10$ of collimator jaw section
 - e_p enhanced by squeezing the beam (30-50% above HL-LHC)**



HRMT-36 (2017)



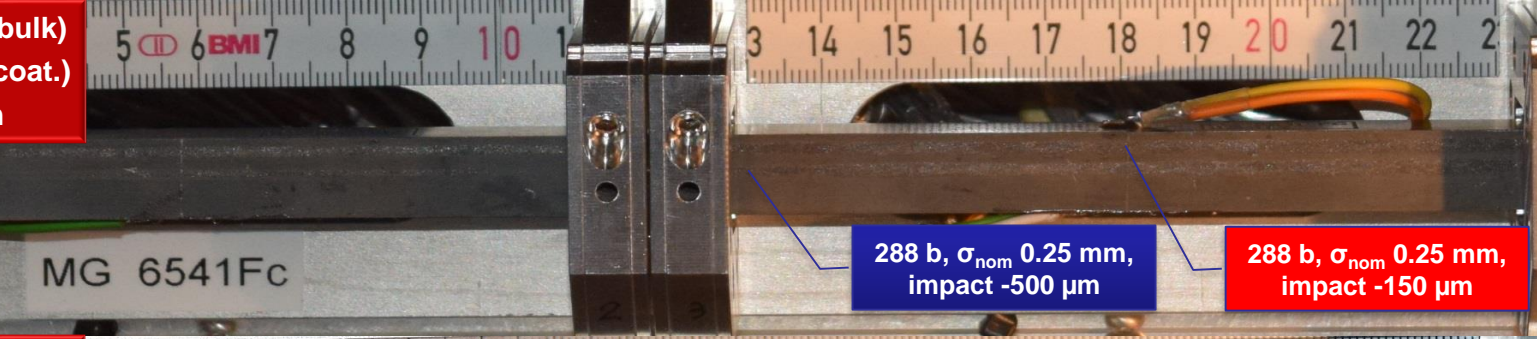
$E_{MAX}=7.68 \text{ kJ/cm}^3$ (bulk)
 $E_{MAX}=15.3 \text{ kJ/cm}^3$ (coat.)
 $\sigma_{real} = 0.29 \times 0.26 \text{ mm}$



144 b, $\sigma_{nom} 0.25 \text{ mm}$,
 impact -150 μm

288 b, $\sigma_{nom} 0.25 \text{ mm}$,
 impact -500 μm

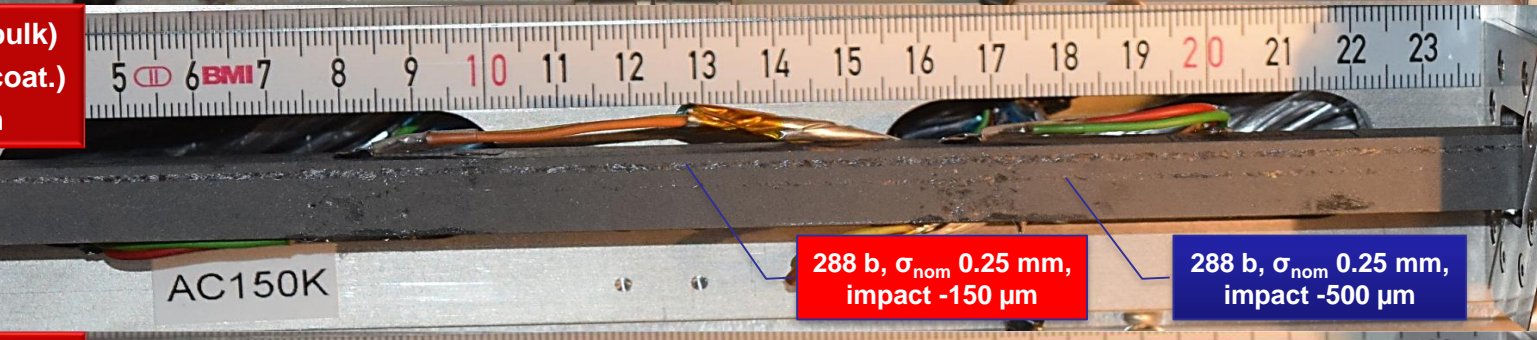
$E_{MAX}=6.11 \text{ kJ/cm}^3$ (bulk)
 $E_{MAX}=13.9 \text{ kJ/cm}^3$ (coat.)
 $\sigma_{real} = 0.29 \times 0.31 \text{ mm}$



288 b, $\sigma_{nom} 0.25 \text{ mm}$,
 impact -500 μm

288 b, $\sigma_{nom} 0.25 \text{ mm}$,
 impact -150 μm

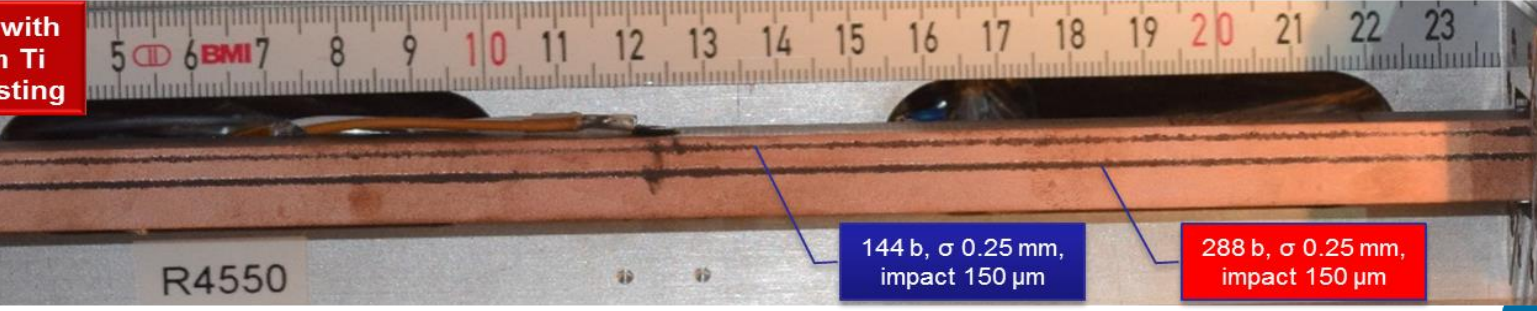
$E_{MAX}=3.72 \text{ kJ/cm}^3$ (bulk)
 $E_{MAX}=14.3 \text{ kJ/cm}^3$ (coat.)
 $\sigma_{real} = 0.38 \times 0.23 \text{ mm}$



288 b, $\sigma_{nom} 0.25 \text{ mm}$,
 impact -150 μm

288 b, $\sigma_{nom} 0.25 \text{ mm}$,
 impact -500 μm

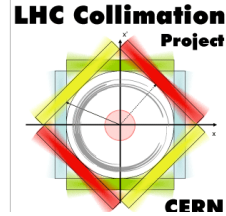
Graphite (R4550) with
 2 μm Cu + 0.5 μm Ti
 coating – CO₂ blasting



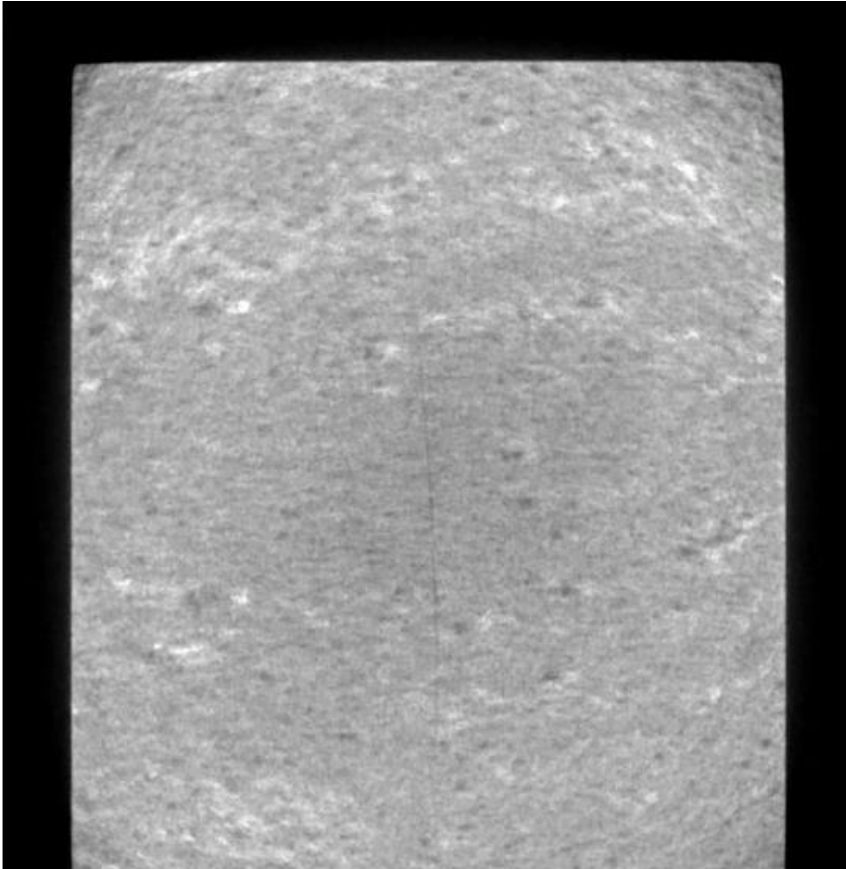
144 b, $\sigma 0.25 \text{ mm}$,
 impact 150 μm

288 b, $\sigma 0.25 \text{ mm}$,
 impact 150 μm

HRMT-36 (2017)



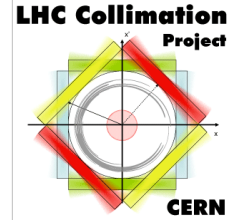
- On top of observing the onset of damage related to e_p (**upstream samples**), onset of damage related to \bar{e}_s (**downstream**) also identified
- Sample section $\sim 1/10$ of collimator block section \rightarrow increased \bar{e}_s



MoGr sample n. 8
(highest average energy density per section)

- Appearing on samples with \bar{e}_s 2.5 higher than HL-LHC accidents
 - Samples with \bar{e}_s equal to HL-LHC \rightarrow below onset of damage
-
- *F. Carra et al. (2017). The “Multimat” experiment at CERN HiRadMat facility: advanced testing of novel materials and instrumentation for HL LHC collimators. J. Phys.: Conf. Ser., Vol 874, Issue 1.*
 - *A. Bertarelli et al. (2018). Dynamic testing and characterization of advanced materials in a new experiment at CERN HiRadMat facility. J. Phys.: Conf. Ser. 1067 082021.*
 - *M. Pasquali et al. (2019). Dynamic response of advanced materials impacted by particle beams: the MultiMat experiment. Submitted to the DYMAT2019 Workshop.*
 - *F. Carra et al. (2019). Mechanical robustness of HL-LHC collimator designs. Accepted in IPAC19, Melbourne, Australia.*

Collimator damage thresholds and accidental scenarios

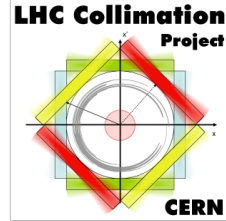


- Damage triggered by e_p (values in the table are in kJ/cm³)

Material	Damage threshold			HL-LHC	Normal case
	1	2	3	4	Beam injection error
CFC	~1.6	Not observed (> 3.8)	Not observed (> 3.8)	—	2.6
Graphite	~2.1	Not observed (> 3.8)	Not observed (> 7.1)	—	Not calculated (> 2.6)
MoGr	—	Not observed (> 7.7)	Not observed (>> 7.7)	—	6.1
Inermet	—	2.5	15.6	35.6	—
CuCD	≤ 2.5	3.6	Not observed (> 13.8)	4.8	—

For coatings: the beam injection error provokes a damage equivalent to threshold 2, but below threshold 3; E_{max} ranging from 12 to 15 kJ/cm³ depending on the coating material and on the substrate

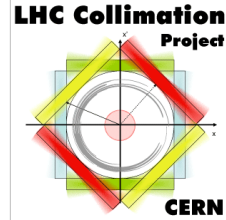
Collimator damage thresholds and accidental scenarios



- Damage triggered by \bar{e}_s (values in the table are in kJ/cm³)

Material	Damage threshold			HL-LHC accidental case	
	1	2	3	Asy. beam dump	Beam injection error
CFC	<i>Not observed (>0.27)</i>	<i>Not observed (>>0.27)</i>	<i>Not observed (>>0.27)</i>	–	0.10
Graphite	<i>Not observed (>0.31)</i>	<i>Not observed (>>0.31)</i>	<i>Not observed (>>0.31)</i>	–	<i>Not calculated (≈0.12)</i>
MoGr	~0.97	<i>Not observed (>>0.97)</i>	<i>Not observed (>>0.97)</i>	–	0.46

Damage levels on SC magnet components



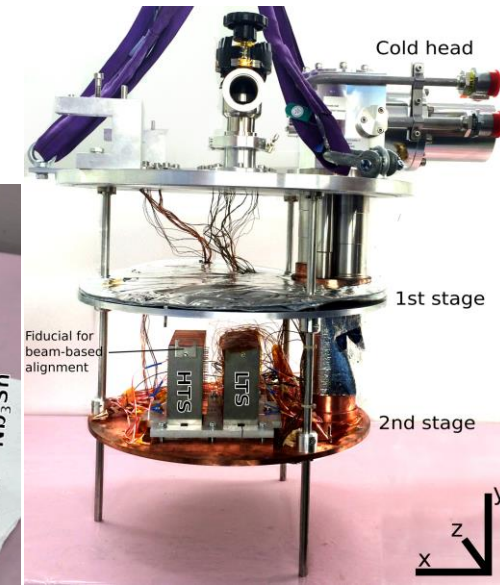
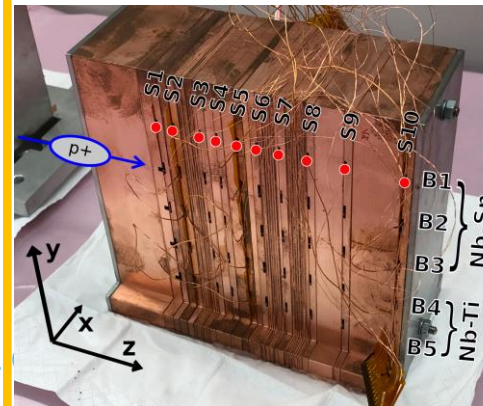
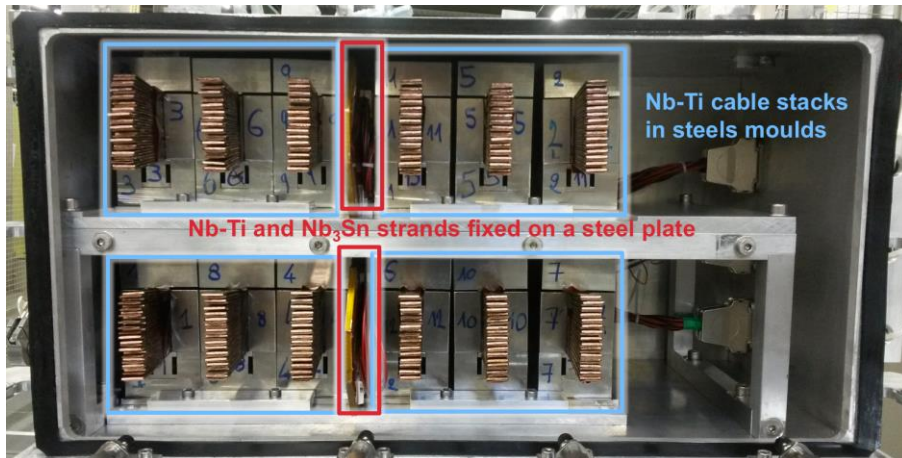
- **Criticality** of injection and dump failures **increases** with increased beam brightness and intensities for HL-LHC, energy deposition up to 100 J/cm^3 expected
- **Study the damage limit** of superconducting magnets components due to beam impact

Room temperature experiment (09.2016):

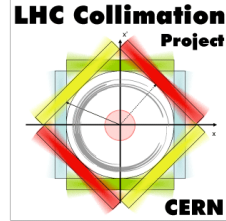
- Nb-Ti & Nb₃Sn strands
- Cable stacks with polyimide insulation
- Up to **2.6e12 p+** per shot @ 440 GeV
- Hotspots up to 1150 K reached in strands

Cryogenic experiment @ **4.5 K** (08.2018):

- Nb-Ti, Nb₃Sn strands & YBCO tapes
- Shots of **3e12 p+** @ 440 GeV
- Hotspots up to **~1250 K** reached in strands



Main results of RT experiment



Polyimide insulation:

- **No degradation** measured after beam impact – temperature up to ~ 1050 K (2.5 kJ/cm³)
- **Weakening** of the insulation at the point of the beam impact was observed for **T > 850 K** (1.9 kJ/cm³)

Nb-Ti strands:

- J_c degradation for hotspot temperatures > **878 K** (2.2 kJ/cm³)

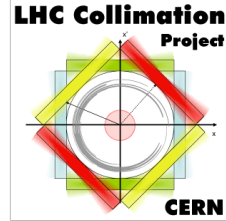
Nb₃Sn strands:

- J_c degradation observed in **all samples** $T \geq 699$ K (1.4 kJ/cm³)

V. Raginel, et al., *First Experimental Results on Damage Limits of Superconducting Accelerator Magnet Components Due to Instantaneous Beam Impact*, IEEE Trans. Appl. SC, Vol 28(4), June 2018

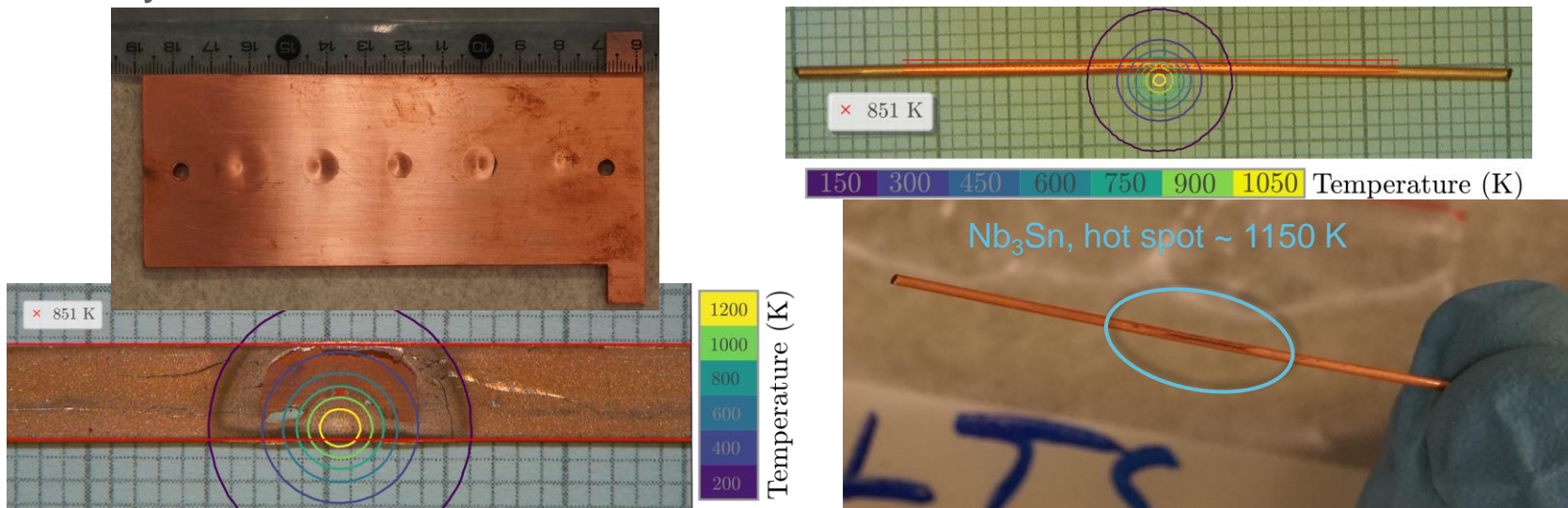
V. Raginel, *Study of the Damage Mechanisms and Limits of Superconducting Magnet Components due to Beam Impact*, CERN-THESIS-2018-090

Observations after cryogenic experiment



- Clear **beam impact marks** on copper blocks of sample holder
- Nb-Ti strands: no visible deformation
- Nb₃Sn strands: **visibly bent** for hotspot temperatures > 700 K (2.2 kJ/cm³), **cracks** in copper matrix
- YBCO tapes: **partial welding** to sample holder for hotspot temperature > 700 K

Critical transport current (I_c) measurements ongoing in collaboration with University of Geneva

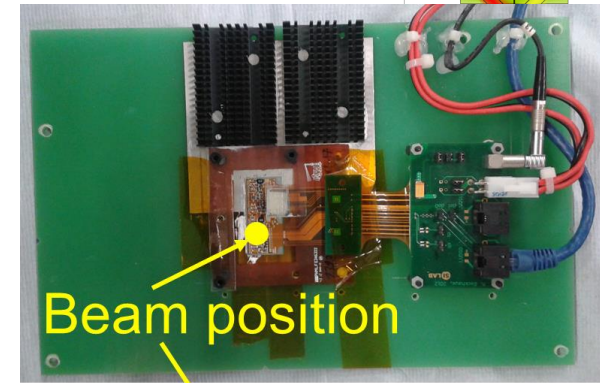


A. Oslandsbotn, A. Will, D. Wollmann, Beam Impact on Superconductor short samples of Nb₃Sn, Nb-Ti and YBCO, 2018, EDMS 2068064

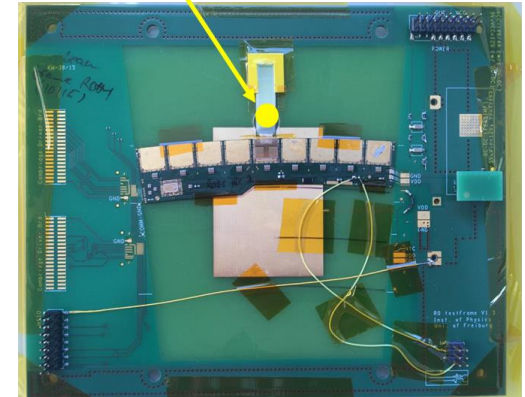
A. Will, et al., Beam impact experiment of 440GeV/p Protons on superconducting wires and tapes in a cryogenic environment, Proceedings of IPAC2019, to be published

ATLAS detectors

- ATLAS silicon tracker detectors: designed to sustain high integrated dose over several years of operation at the LHC. The upgrade of LHC to higher luminosity (HL-LHC) calls for new tests.
- HL-LHC failure scenarios: asynchronous beam dump or wrong injection settings.
- Inner tracker (ITk) will be entirely in Si. Latest tests under beam impact performed in July 2018.



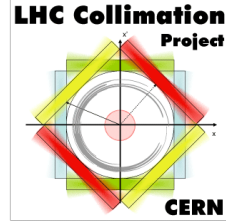
ITk DAQLoad



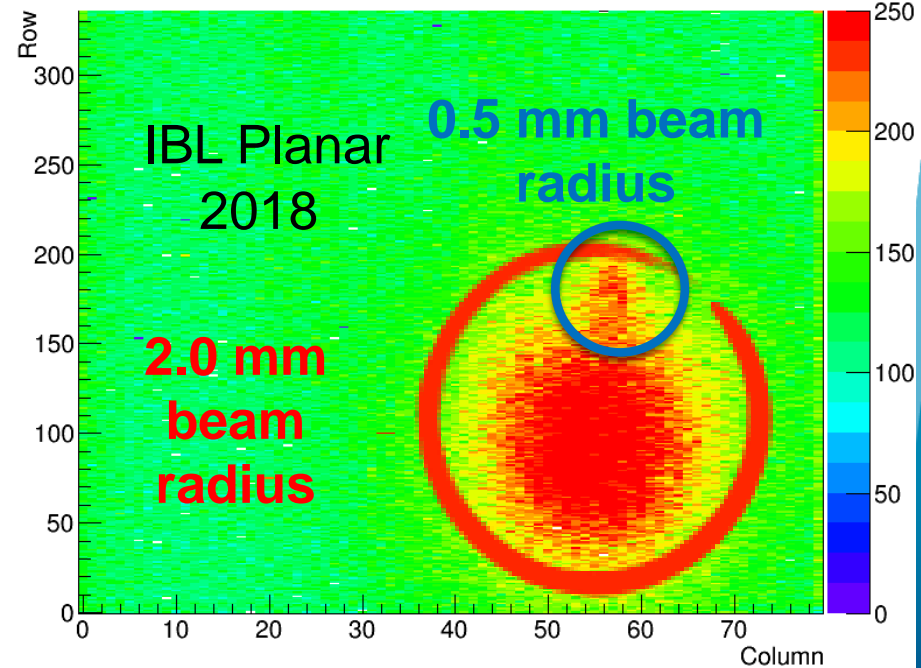
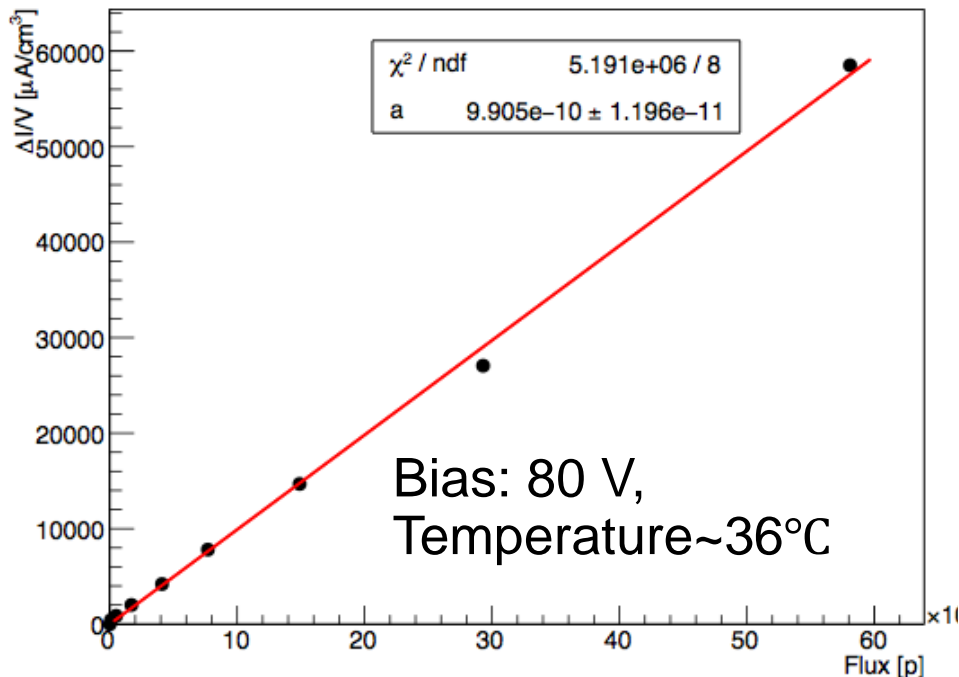
- ITk strip miniature sensor available for the beam test. ITk Pixel prototype with RD53A not available at that time, used most advanced technology IBL.
- Improved cooling system via aluminium and dissipator: $T \sim 36^{\circ}\text{C}$

Module	IBL	ITk
Type	n^+ -in-n, Planar	n^+ -in-p, Low-R
Chip	FE-I4	ABC130
Total Size	2x4 cm ²	0.7x2.6 cm ²
Thickness	200 μm	310 μm
Channel/pitch	2x26680 (50x250 μm ²)	64 (77 μm)
Max. Dose	250 MRad	35 MRad

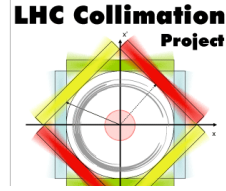
ATLAS detectors: IBL results



- Module tested in Stable beam configuration.
- Bulk and surface damage post-irradiation, cause a linear increase of the leakage current with the fluence.
- Monitoring of leakage current after each shot. Increase after irradiation: $\sim 230 \mu\text{A}$ at 80 V.
- Noise increases around the beam spot in a similar way for the three modules.
- Limit on the damage threshold from $300 \cdot 10^{10} \text{ p/cm}^2$ ([2006](#)) to $1 \cdot 10^{13} \text{ p/cm}^2$ ([2017/18](#)).

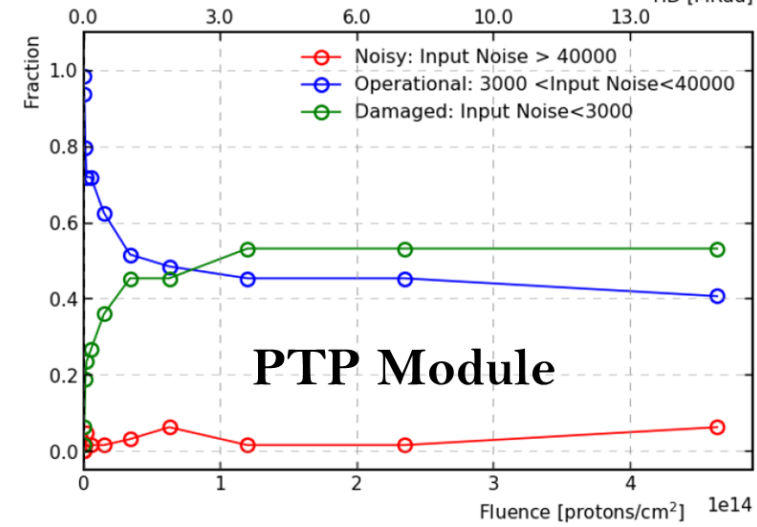


ITK STRIP: Influence on Read-out Electronics



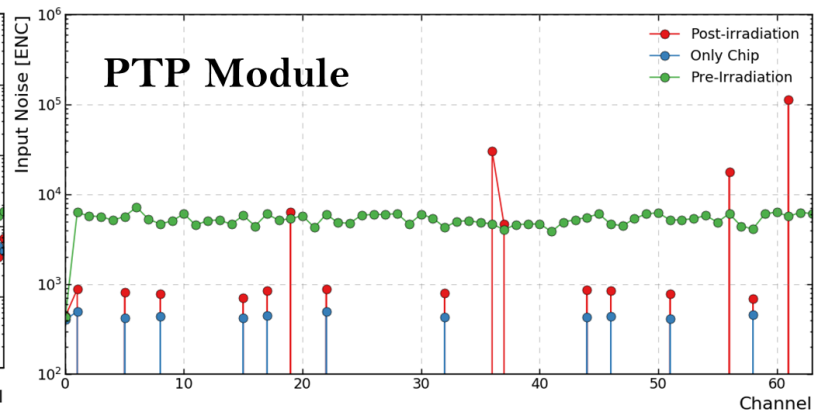
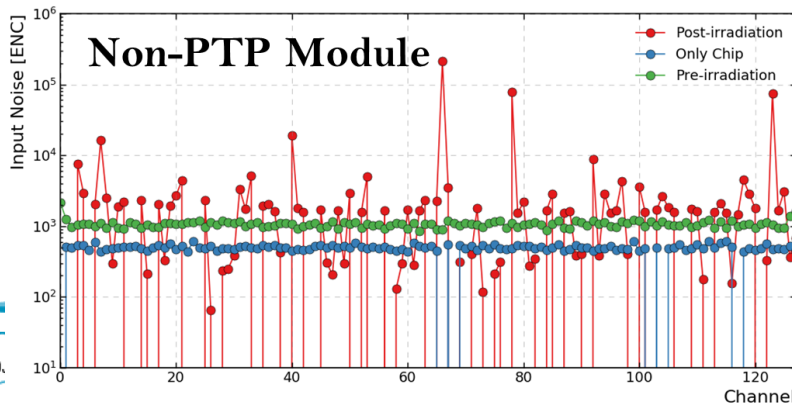
PTP Module:

- Module noise increase concentrated in the first shot
- Stable behavior before $1 \cdot 10^{13}$ proton (3 MRad)
- With increase of the proton fluence, a decreasing number of fully operating channels was observed
- **After about $6 \cdot 10^{13}$ protons (15 MRad) more than 50% of channels have been damaged for the PTP module**



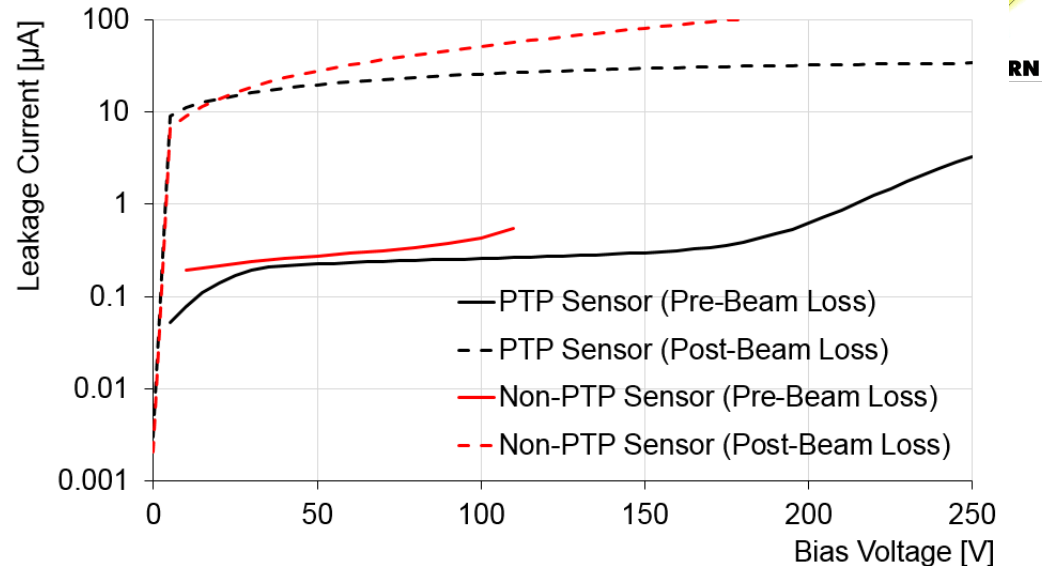
Non-PTP Module:

- Unfortunately, due to connectivity problems during the experiment, the on-line monitoring of this sensor was not possible
- Noise and gain measurements before and after the beam-loss experiment showing typical values for silicon strip modules
- **Apparently no damage of beam-loss on the read-out channels for the non-PTP module**



ITK STRIP: Influence on Read-out Electronics

- After the beam-loss experiment, the sensors were disassembled from the testing modules and characterized
- Typical behavior of irradiated sensors

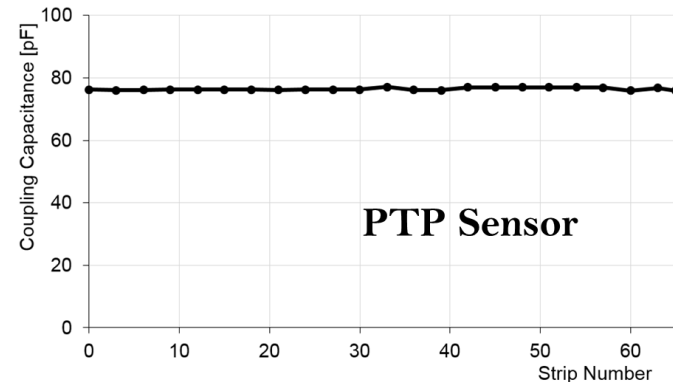
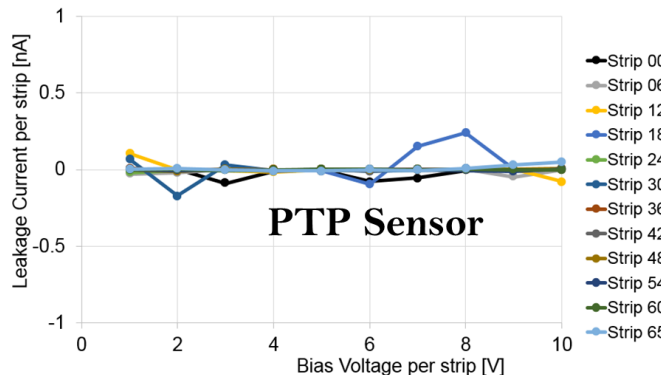


PTP Sensor:

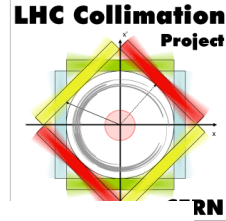
- Measured current across oxide and value of coupling capacitance:
 - ✓ Strip current: OK → No electrical continuity across coupling oxide
 - ✓ Coupling capacitance: OK → Expected value, no variation across the sensor

Non-PTP Sensor:

- Measurement of current across oxide showing 70% of strip coupling capacitors broken **Non-PTP strips have not survived the beam-loss experiment**

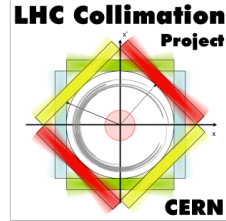


Conclusions



- The damage mechanism in case of particle beam impact on a material is controlled by two parameters: **peak energy density (\bar{e}_s)** and **maximum energy over a longitudinal cross-section (e_p)**
- However, **damage definition changes depending on the application**: it may be related to the thermostructural behaviour (collimators), to the degradation of the relevant electromagnetic properties (SC magnets), or to a loss of electronic functionality (ATLAS detectors)
- Need of performing **experimental tests** (HiRadMat) and, where possible, **numerical simulations**, combining the two methods
- For **collimators**, dedicated tests aimed at simulating similar or higher expected in the accidental scenario.
 - For primary and secondary collimator materials, **thresholds 2 and 3 have never been reached so far**
 - For tertiary collimator materials, **threshold 3 is expected in the case of tungsten under energies lower than the accidental scenario**. In the case of CuCD, threshold 3 is **not reached neither in the accidental scenario, nor experimentally**

Conclusions



- The tests done in 2016 and 2018 to **SC magnet components** allowed:
 - Assessing the damage thresholds for the **insulation**
 - Evaluate the behaviour and damage limits of **different SC solutions: Nb-Ti, Nb₃Sn and YBCO**
 - Effects on the **superconducting properties** (I_c) under checking
- Technical solutions for the **ATLAS detectors** also recently tested.
 - Allowed to choose between **different technologies**. For example, highlighted the need of a PTP system.
 - **Updated damage thresholds**, first defined in 2006.

- In the experimental tests, in spite of the lower beam stored energy, the expected damage mechanisms was mimicked through squeezing the HRMT beam, changing the sample geometry.
- **However, to completely validate full scale devices and derive upper damage thresholds, it is of paramount importance to perform tests with the nominal LIU/HL-LHC beam stored energy.**



***Thanks for your
attention!***





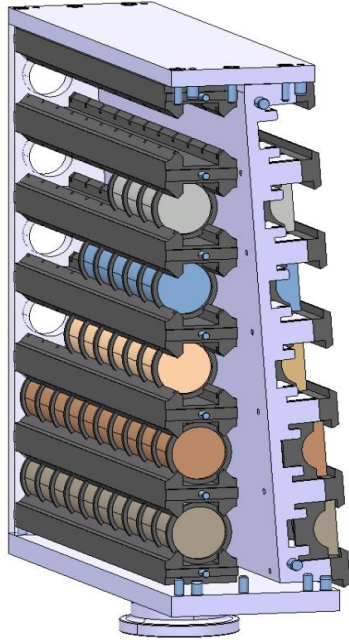
Backup slides



HRMT-14 (2012)

- Test of specimens from 6 different materials: Inermet180, Mo, Glidcop, MoCuCD CuCD, and MoGr (very old grade with high density, 5.4 g/cm^3)
- Allowed characterization of materials of interest for collimators
- Tuning of numerical models, with very good benchmarking between measurements and simulations

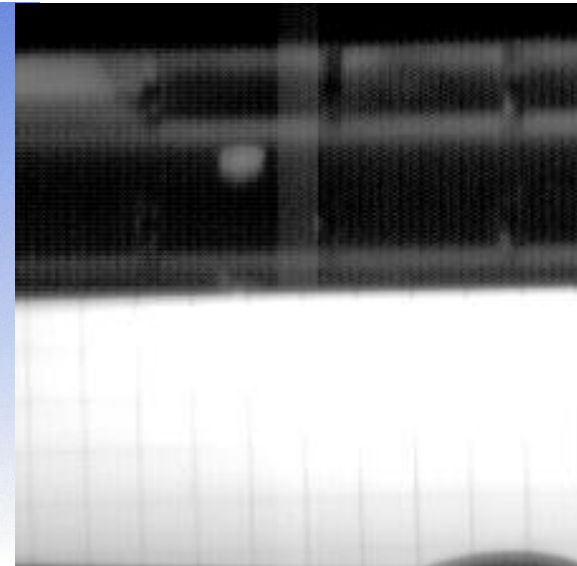
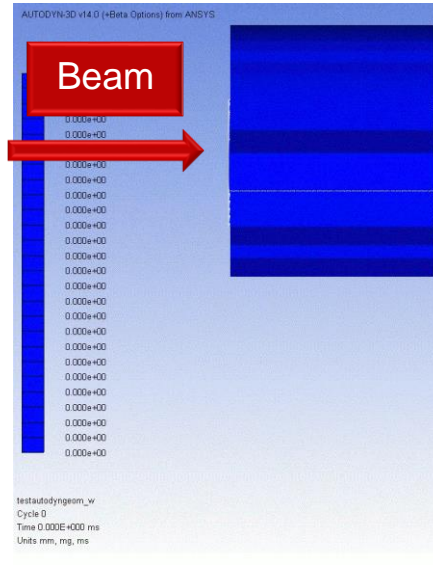
Medium Intensity Samples (Type 1)



- Strain measurements on sample outer surface;
- Radial velocity measurements (LDV);
- Temperature measurements;
- Sound measurements.

High Intensity Samples (Type 2)

- Strain measurements on sample outer surface;
- Fast speed camera to capture fragment front formation and propagation;
- Temperature measurements;
- Sound measurements.

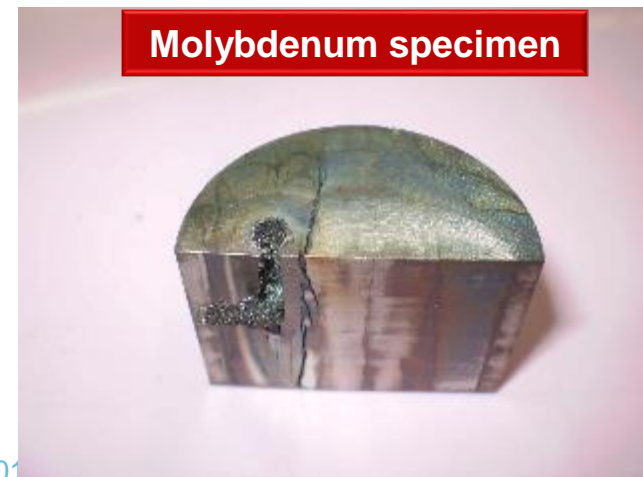
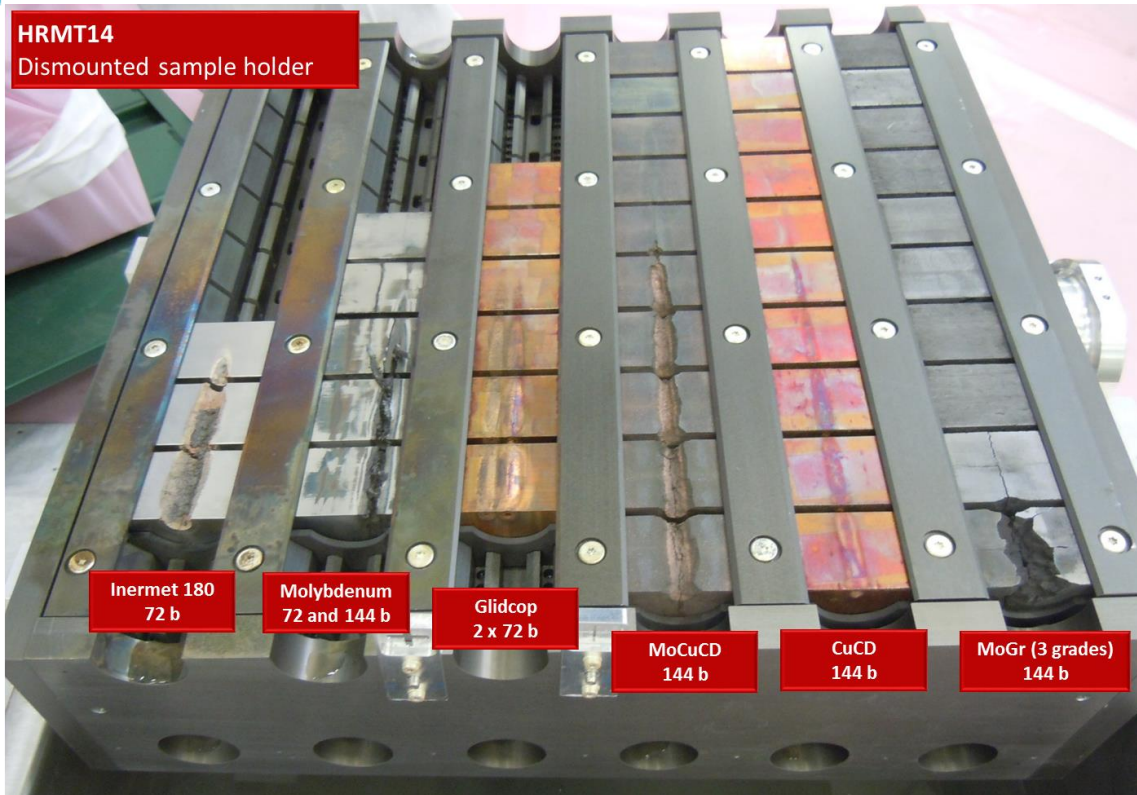


Case	Bunches	p/bunch	Total Intensity	Beam Sigma	Specimen Slot	Velocity
Simulation	60	1.5e11	9.0e12 p	2.5 mm	9	316 m/s
Experiment	72	1.26e11	9.0e12 p	1.9 mm	8 (partly 9)	~275 m/s

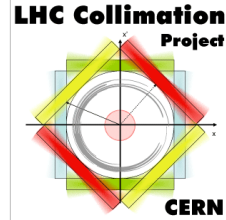
- A. Bertarelli et al. (2013). An experiment to test advanced materials impacted by intense proton pulses at CERN HiRadMat facility. Nucl. Instr. Meth. Phys. Res. B 308:88–99.

HRMT-14 (2012)

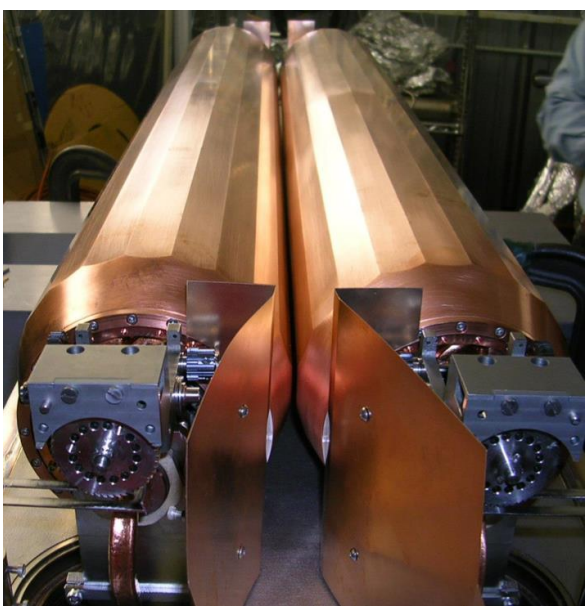
- Tank opened in **May 2015** in b. 109 (CERN), after 2 ½ years of cool-down
- Activation was low, but **risk of contamination** due to radioactive fragments and powders (mostly Cu and W)
- Non-destructive and destructive testing campaign



HRMT-21 (2017)



- Test on **SLAC rotatable collimator** (Glidcop)
- Low-impedance secondary collimator** capable of withstanding 7 TeV failures
- Goals:
 - Demonstrate that the rotation functionality works for the design failure at top energy (Asynchronous beam dump: **8 bunches @ 7 TeV**)
 - Understand onset of damage for even more demanding scenarios, e.g. LHC injection error: **288 bunches @ 450 GeV**
 - Integrity control of the cooling pipes under both impact and jaw rotation
 - Check the eventual sticking of the jaws in case of ejecta with LHC-type aperture



Beam Pulse List									
No	Intensity			Beam spot [mm]		Bunch spacing [ns]	Pulse length [μs]		
	# bunches	p/bunch	Total	Sigma_x	Sigma_y				
1-25	1	6.00E+10	3.00E+12	0.35	0.35	25	0.025	Alignment	
26	6	1.20E+11	7.20E+11	0.35	0.35	25	0.15	Shot #1	Rotation
Rotation of 1 facet AC (~1.5 hours)									
27-51	1	6.00E+10	3.00E+12	0.35	0.35	25	0.025	Alignment	
52	12	1.20E+11	1.44E+12	0.35	0.35	25	0.3	Shot #2	Rotation
Rotation of 1 facet AC (~1.5 hours)									
53-77	1	6.00E+10	3.00E+12	0.35	0.35	25	0.025	Alignment	
78	24	1.20E+11	2.88E+12	0.35	0.35	25	0.6	Shot #3	Rotation
Rotation of 1 facet AC (~1.5 hours)									
79-103	1	6.00E+10	3.00E+12	0.35	0.35	25	0.025	Alignment	
104	36	1.20E+11	4.32E+12	0.35	0.35	25	0.9	Shot #4	Rotation
Rotation of 1 facet AC (~1.5 hours)									
105-129	1	6.00E+10	3.00E+12	0.35	0.35	25	0.025	Alignment	
130	48	1.20E+11	5.76E+12	0.35	0.35	25	1.2	Shot #5	Rotation
Rotation of 1 facet AC (~1.5 hours)									
131-155	1	6.00E+10	3.00E+12	0.35	0.35	25	0.025	Alignment	
156	72	1.20E+11	8.64E+12	0.35	0.35	25	1.8	Shot #6	Rotation
Rotation of 5 facet AC + 1 facet BD (~9 hours)									
157-181	1	6.00E+10	3.00E+12	0.35	0.35	25	0.025	Alignment	
182	144	1.20E+11	1.73E+13	0.35	0.35	25	3.6	Shot #7	Rotation
Rotation of 5 facet AC + 5 facet BD (~15 hours)									
183-207	1	6.00E+10	3.00E+12	0.35	0.35	25	0.025	Alignment	
208	288	1.20E+11	3.46E+13	0.35	0.35	25	7.2	Shot #8	
Total				9.96E+13				Total ~31.5 hours	

Equivalent total energy

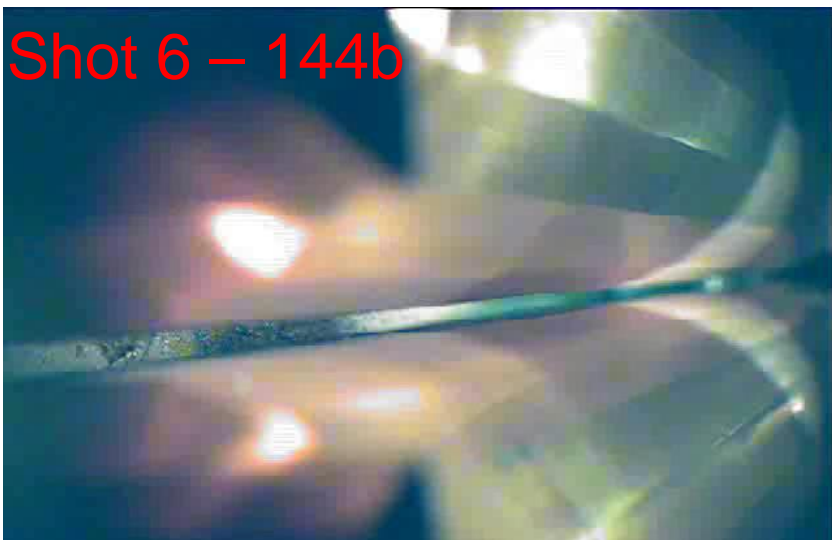
Onset of plastic damage
estimated to be around
2E12p @ 440GeV (141kJ)

Intermediary shots

Design failure at 7TeV
15E12p @ 440GeV (1MJ)

HL-LHC injection error
3.5E13p @ 440GeV (2.4MJ)

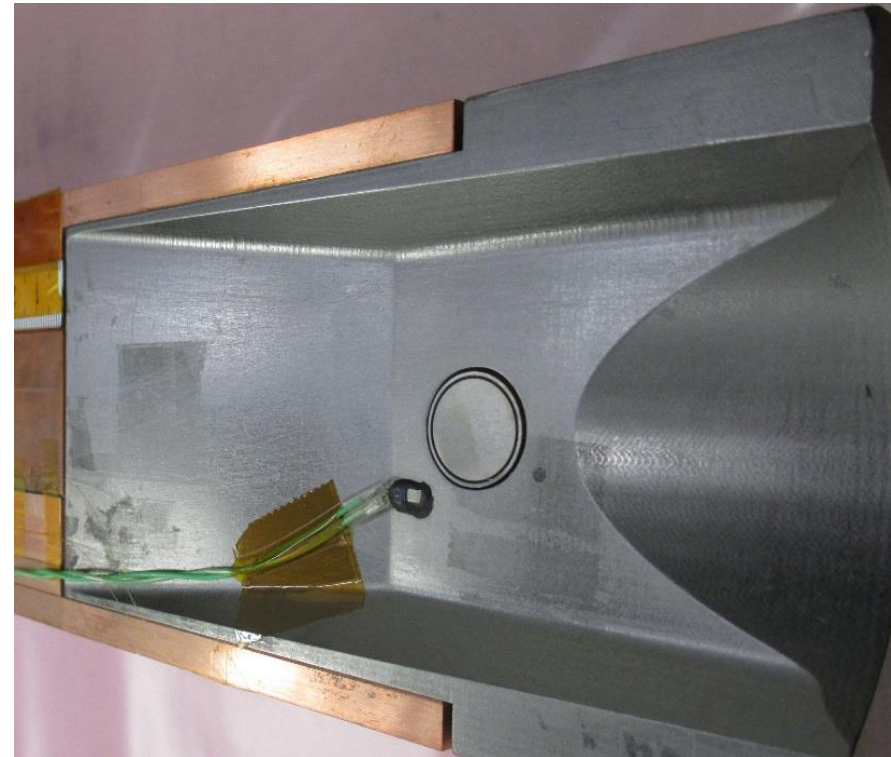
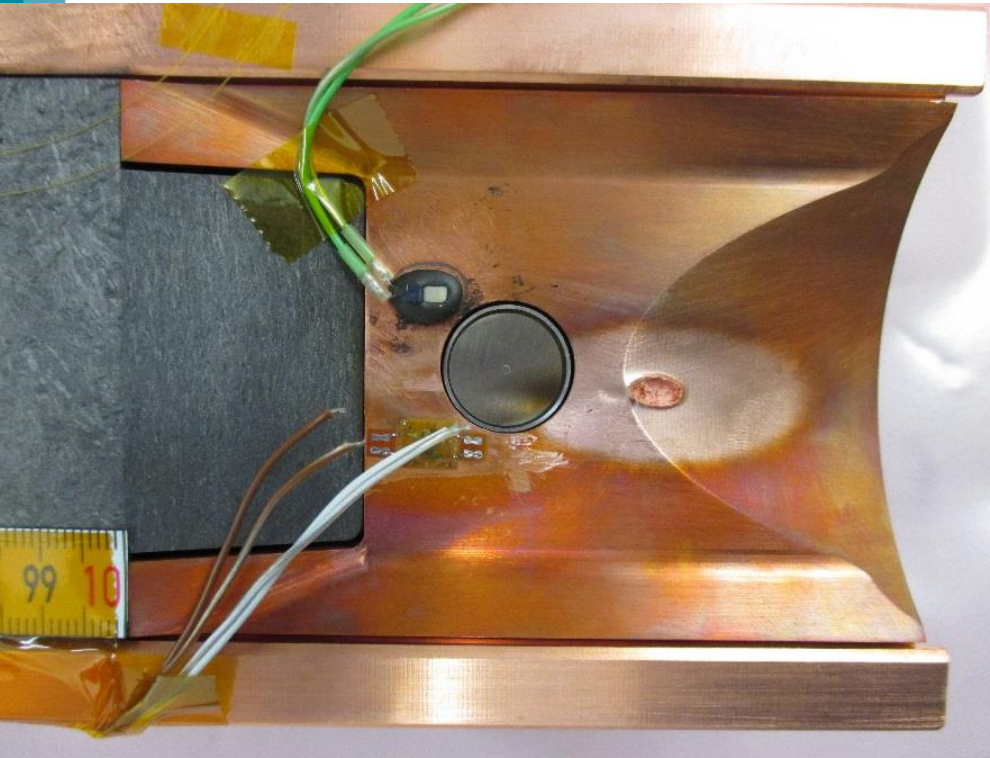
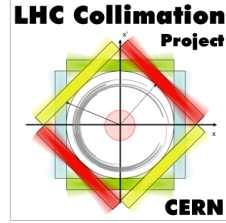
HRMT-21 (2017)



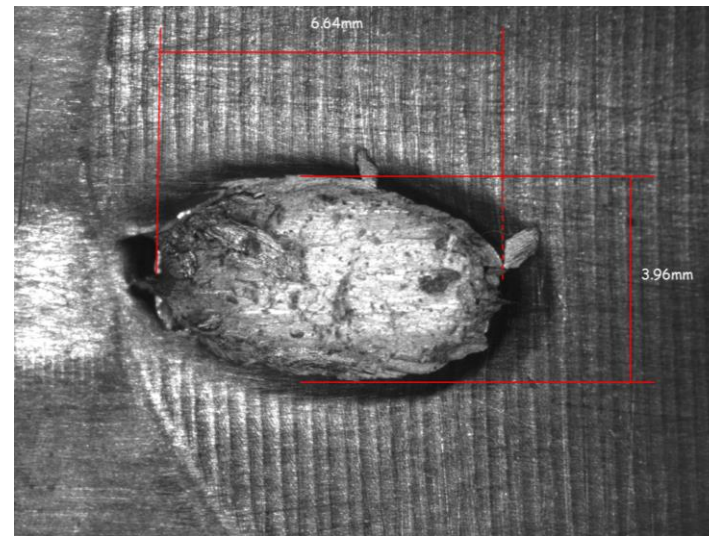
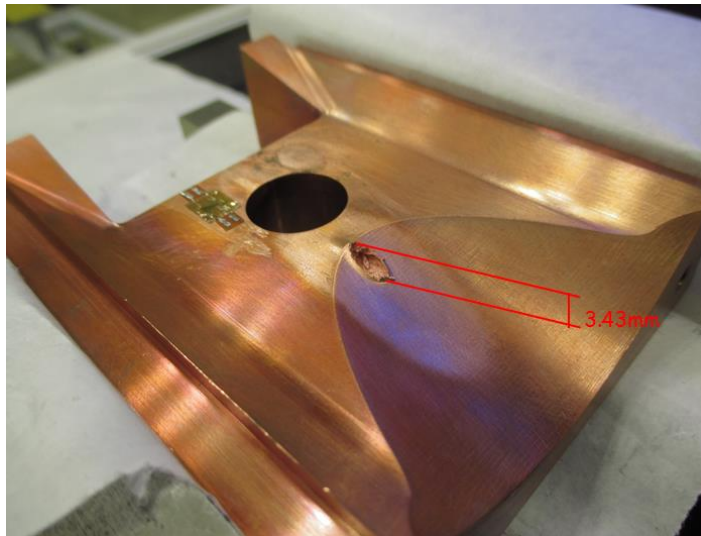
- G. Valentino et al. (2019) Design, construction and beam tests of a rotatable collimator prototype for high-intensity and high-energy hadron accelerators. *Collimation in Proton and Neutron Accelerators*



HRMT-23 (2015)



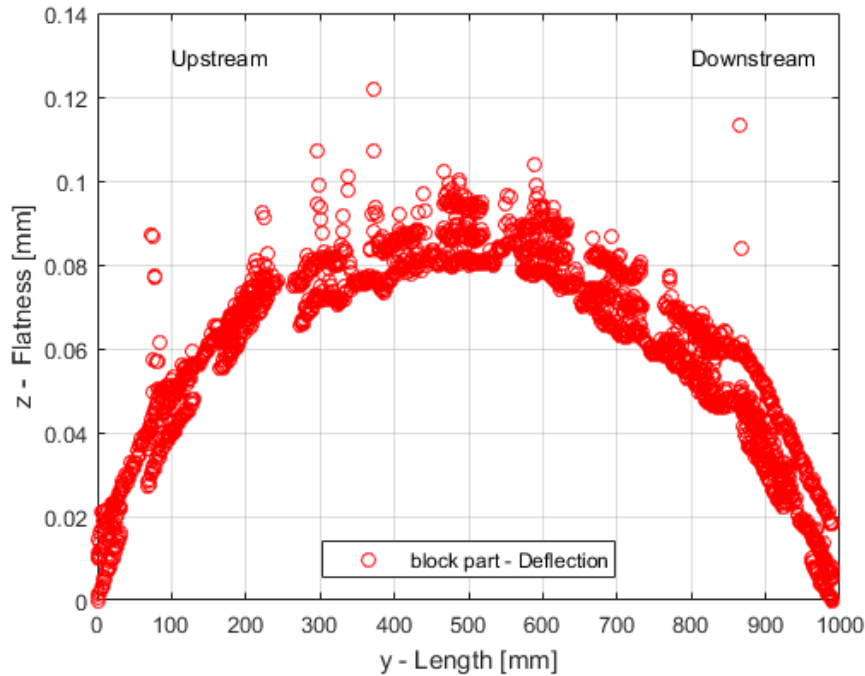
Metrology - Taperings



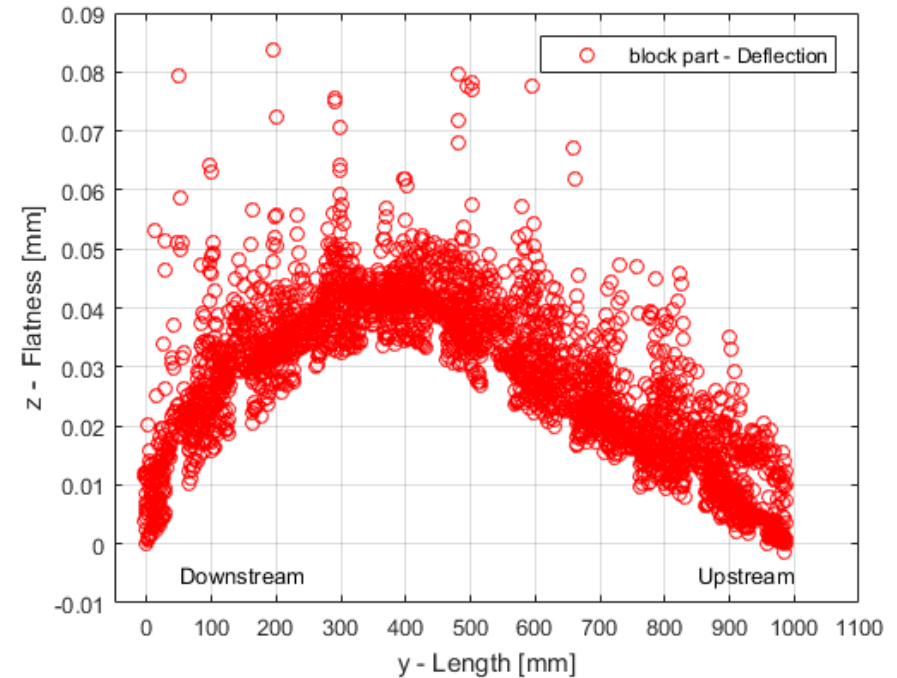
Downstream **Glidcop tapering** of CFC jaw **locally melted**
MoGr no damage detected

Metrology – MoGr and CuCD jaws

MoGr → ~80 μm



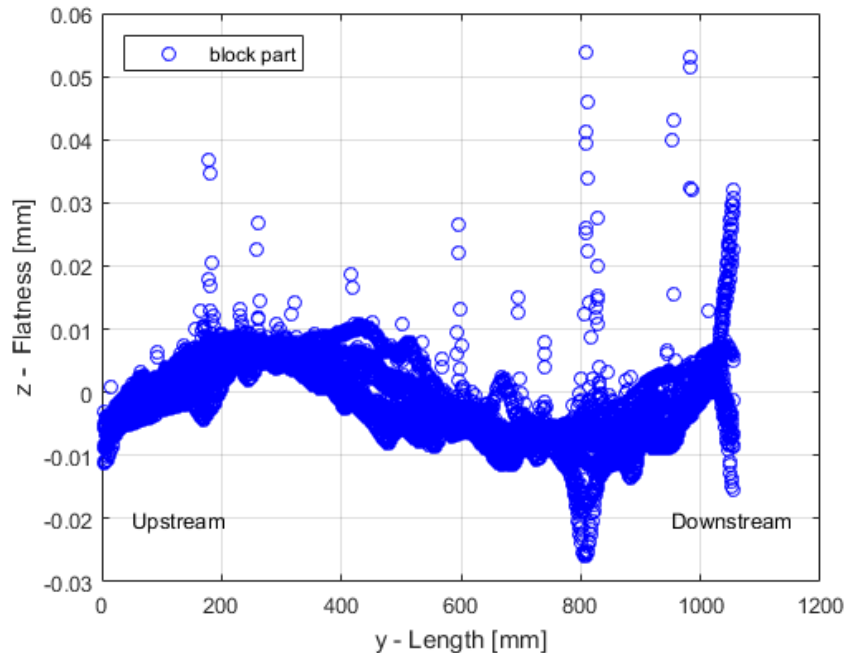
CuCD → ~50 μm



Plastic deformation? Yes → most likely due to a cumulative effect of successive shots with energy equal/above the accidental case scenario

Metrology – CFC jaw housing

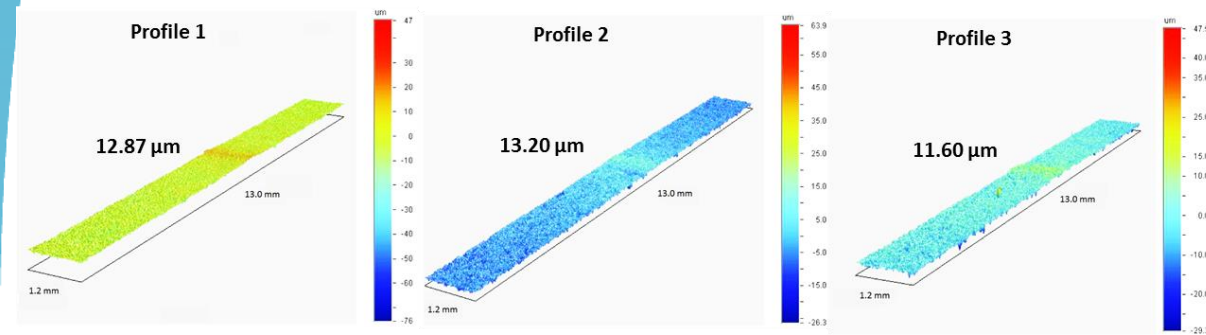
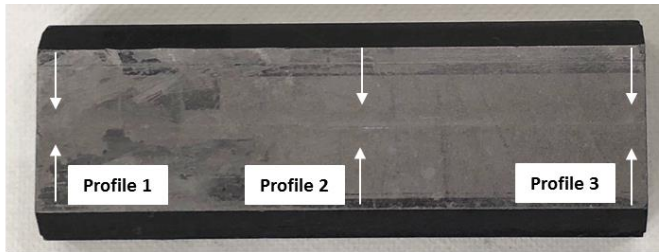
CFC → ~20 μm



Flatness within the machining tolerance → CFC lower energy absorption

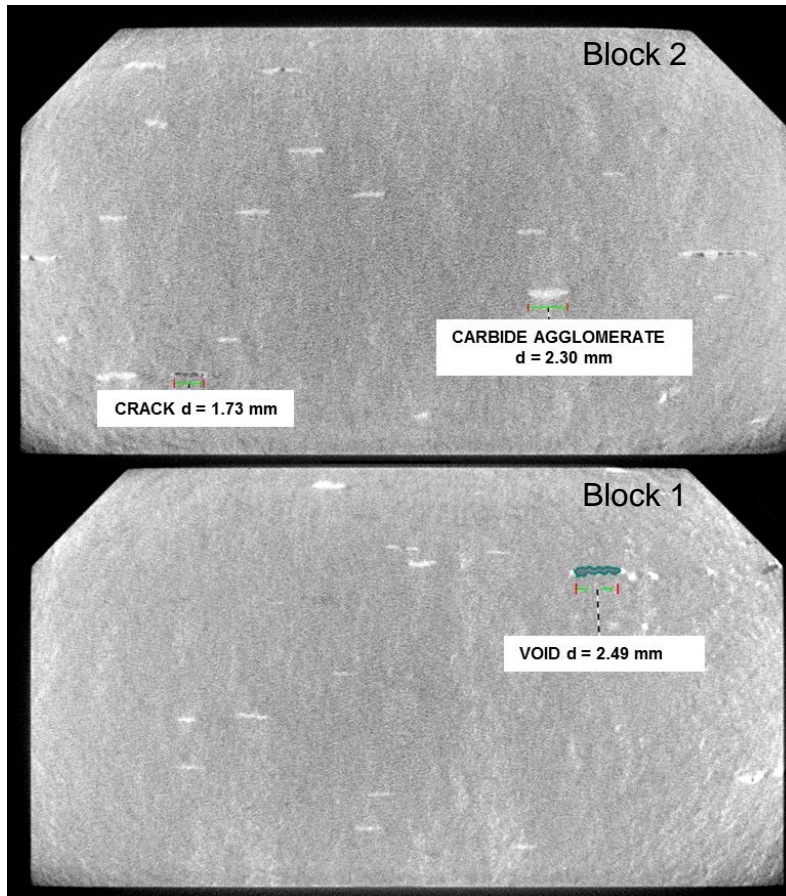
3D topography - MoGr

Block 2



- No spallation takes place \rightarrow pseudo-plastic expansion
- Defect height is in the range of **12-13 μm** and localized in tenth of mm width region
- Surface roughness $1.5 \mu\text{m}$ \rightarrow considered as mean error of the height measurements

Computed tomography - MoGr

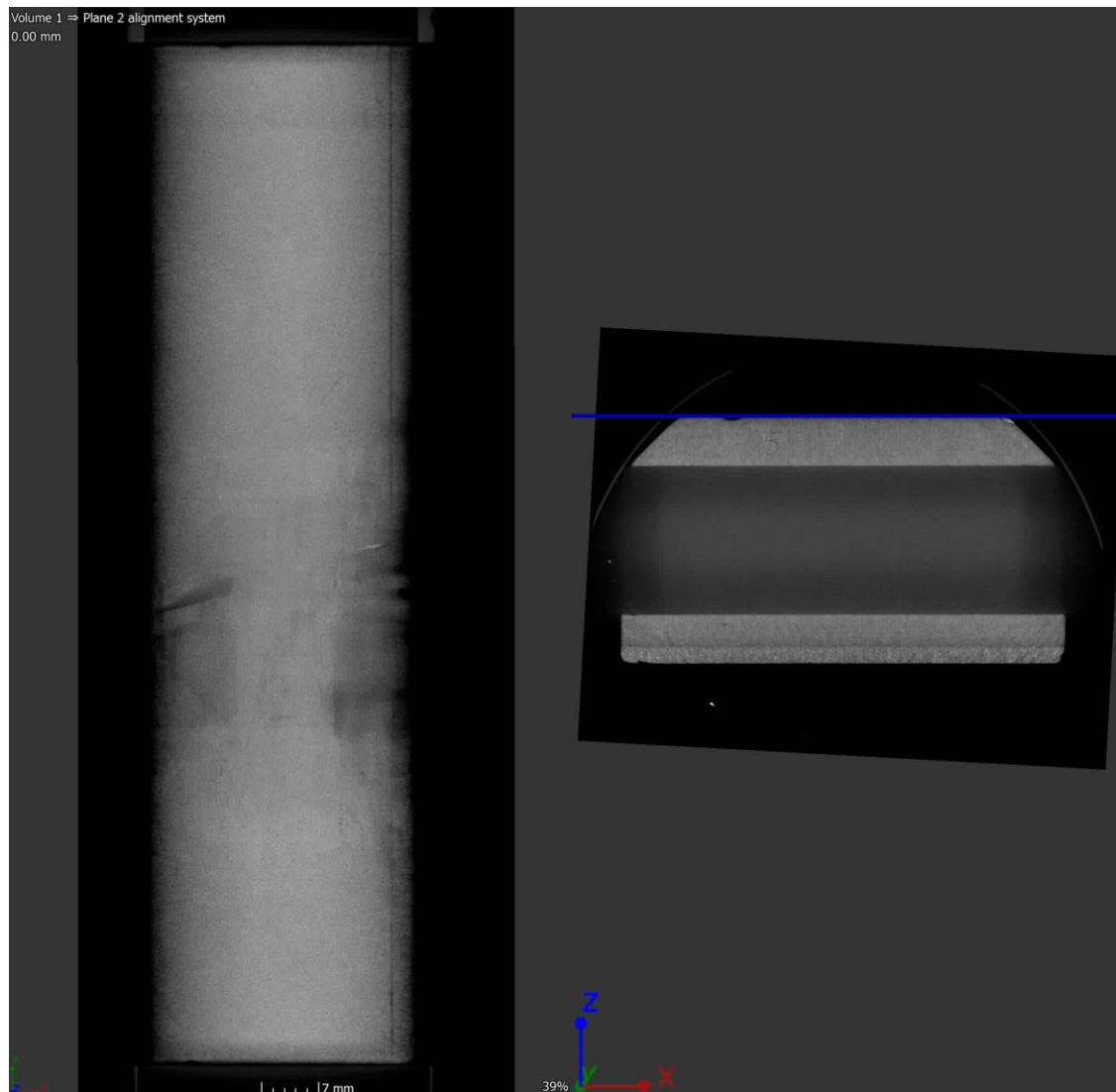


- No internal damages detected
- Agglomerate of molybdenum carbides with disk shape, dimensions few mm
- Small cracks or voids appear in correspondence of carbide agglomerates randomly distributed in the bulk → not attributed to beam effect



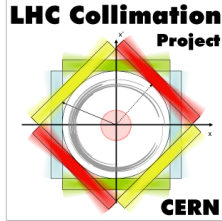
Production process not optimized yet at the time of the experiment

Computed tomography - MoGr



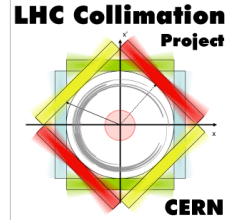
- Last block

Useful links and literature



- **MoGr production management:**
 - EDMS [CERN-0000186962](#)
- **Procedures for UHV compatibility of MoGr**
 - Vacuum firing on uncoated MoGr, EDMS n. [2050564](#)
 - Surface preparation and vacuum firing on MoGr to be coated, EDMS n. [2067775](#)
 - Thermal treatment on MoGr post-coating, EDMS n. [2083915](#)
- **Irradiation studies on materials:**
 - Summary of irradiations at BNL and Kurchatov Institute for MoGr and CuCD: Eucard-2 deliverable [D11.3](#): “Irradiation tests results”, 2018
 - MoGr irradiation with ions at GSI:
 - “Heavy ion induced radiation effects in novel molybdenum-carbide graphite”, [GSI Scientific report](#), 2015
 - “Present results on material damage from irradiation”, Eucard-2 milestone [MS70](#), 2015
 - “Radiation induced effects in MoGr composites”, [Eucard2 WP11 meeting](#), Malta, 2016
 - CFC irradiation at Kurchatov Institute: “The effects of high-energy proton beams on LHC collimator materials”, Kurchatov final technical report, 2008

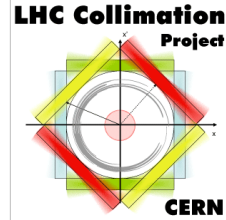
Thermomechanical tests



Property	Specification			Batch 2	
	II*	I	Unit	II*	I
Density at 20°C	2.40 – 2.60		[g/cm ³]	2.59	
Specific heat at 20°C	>0.6		[J/(g·K)]	0.65	
Electrical conductivity at 20°C	>0.90		[MS/m]	1.02	
Thermal Diffusivity 20°C /at 300°C	>390/120	>25/8	[mm ² /s]	407/115	17/5
Thermal conductivity at 20°C /at 300°C	>500/300	>35/25	[W/(m·K)]	705/333	29/15
Coefficient of thermal expansion 20-1000°C	<2.9	<15	[10 ⁻⁶ K ⁻¹]	2	16.3
Young's Modulus at 20°C	35<E<70	5<E<8	[GPa]	85	5.2
Flexural strength at 20°C	>60	>10	[MPa]	89	13.7
Flexural strain to rupture at 20°C	>2500	>4000	[μm/m]	1450	4100
Dimensional stability	<0.05	<0.25	%	0	0.03

Figures of merit	Baseline	Batch 2
TRI	160	255
TSI	38	68
RFI	0.95	1.01

Thermomechanical tests



Property	Specification			Batch 2	
	II*	I	Unit	II*	I
Density at 20°C	2.40 – 2.60		[g/cm ³]	2.55	
Specific heat at 20°C	>0.6		[J/(g·K)]	0.63	
Electrical conductivity at 20°C	>0.90		[MS/m]	0.85±0.03	
Thermal Diffusivity 20°C /at 300°C	>390/120	>25/8	[mm ² /s]	340/95	29/8
Thermal conductivity at 20°C /at 300°C	>500/300	>35/25	[W/(m·K)]	527/306	47/25
Volumetric CTE 20-1000°C	<7		[10 ⁻⁶ K ⁻¹]	5.8	
Coefficient of thermal expansion 20-1000°C	<2.9	<15	[10 ⁻⁶ K ⁻¹]	2.5	12.4
Young's Modulus at 20°C	35<E<70	5<E<8	[GPa]	67.4	5.2
Flexural strength at 20°C	>60	>10	[MPa]	70.3	13.7
Flexural strain to rupture at 20°C	>2500	>4000	[µm/m]	2000	4100
Dimensional stability	<0.05	<0.25	%	0.02	0.2

Figures of merit	Baseline	Batch 2
TRI	160	266
TSI	38	59
RFI	0.95	0.95